Metallic behavior of Pd atomic clusters

F. Aguilera-Granja

Instituto de Física "Manuel Sandoval Vallarta". Universidad Autónoma de San Luis Potosí, S.L.P. 78000, México

A. Vega

Departamento de Física Teórica, Atómica, y Óptica. Universidad de Valladolid, E-47011 Valladolid, Spain

J. Rogan

Departamento de Física, Facultad de Ciencias. Universidad de Chile, Casilla 653, Santiago 1, Chile

G. García

Facultad de Física. Universidad Pontificia Católica de Chile, Casilla 306, Santiago, Chile, 7820436

(Dated: June 20, 2007)

We report a study of the nonmetal-metal transition of free-standing Pd_N clusters ($2 \leq N \leq 21$) carried out through two different theoretical approaches that are extensively employed in electronic structure calculations: a semi-empirical Tight-Binding (TB) model and an *ab-initio* DFT pseudopotential model. The calculated critical size for the metallic transition decreases fast with the temperature and an oscillatory dependence with the cluster size is obtained particularly in the DFT approach. TB model describes well the metallic behavior for cluster sizes beyond $N \approx 12$. Our obtained critical size at room temperature is of the order of the experimental estimation.

Keywords: DFT methods, Tight-Binding methods, metallic behavior, nonmetal to metal transition in transition-metal clusters

I. INTRODUCTION

The insulator to metal transition in atomic clusters as a function of their size is of fundamental interest from both the scientific and technological points of view. The discrete spectrum of the electronic states will begin to form a quasi-continuous band for a critical cluster size depending on the temperature. Although this question was originally addressed by Fröhlich seventy years ago,[1] it is still far from being completely understood. From the technological point of view, the insulator or the metallic character of an atomic cluster is also of great relevance, particularly in the context of transport properties in nanostructures and nanocontacts,[2,3] where it is very important to determine and to predict if the transport is tunneling-like or through molecular states extending through the entire cluster or molecule. The insulator to metallic transition may appear at some critical size when increasing the degree of miniaturization of microelectronic devices.

The nonmetal to metal transition in clusters has been studied experimentally by several groups and through different techniques.[4–8] In general, for clusters of $3d$ and $4d$ elements this transition is experimentally observed at about $N \approx 50$ atoms at low temperature (77 K liquid nitrogen) or at smaller sizes at room temperature. For the theoretical description of the metallic behavior, it is necessary to accurately determine the location of the electronic states close to the Fermi level, for which the optimization of the cluster geometry is essential due to the interplay between the electronic structure and the atomic environment. This transition has been studied for some transition metal clusters by several authors[9–15]

using Kubo's criterium[16], which establishes that a system becomes metallic when the density of states (DOS) at the Fermi level exceeds the $1/k_B T$.

In the particular case of Pd clusters, experimental results by Aiyer and coworkers[5] indicate that, at room temperature, clusters of $N \approx 50$ are in the threshold to undergo the nonmetal to metal transition. Further support to this indication is provided by the different reactivity of the Pd_{50} in comparison with larger Pd clusters, as well as by Wertheim's experimental measurements on core-level binding energy shift.[4] Pd is a very interesting element in many respects. It is in the frontier of the magnetism (a magnetic moment has been observed in clusters despite the paramagnetic character of the bulk) and its suitability for catalytic devices has been demonstrated.[17]

It is our aim here to perform a systematic study of the nonmetal-metal transition in free-standing Pd_N clusters ($2 \leq N \leq 21$) using two different theoretical approaches that are extensively employed in electronic structure calculations. We have used, on the one hand, the *ab-initio* pseudopotential DFT calculation, as implemented in the SIESTA code,[18] and on the other hand a self-consistent real space *spd* TB method.[12,19,20] As a first step, a set of possible geometrical structures for each cluster size are determined using a Genetic Algorithm[21–24] (GA) on a phenomenological Gupta potential,[26] and then re-optimized with conjugate gradients as implemented in the SIESTA code. The metallic behavior of those structures is studied using both SIESTA and TB since it has been also our purpose to benchmark both theories.

The paper is organized as follows, in Section II we briefly present the theoretical models. Section III is devoted to present and discuss the results and Section IV summarizes our main conclusions.

II. COMPUTATIONAL METHODS

A. Genetic Algorithm

In order to search the minimum energy cluster structure we use a genetic algorithm (GA), which is a global search technique based on the principles of natural evolution[21–24]. It uses operators that are analogues to evolutionary processes of mating or crossover, mutation and natural selection, to explore the multidimensional parameter spaces.

In particular, we implemented a GA that uses real numbers (the coordinates of each atoms) instead of a binary representation in order to represent each cluster. In the GA scheme each cluster represents a trial solution of the problem and corresponds to an individual. The initial population corresponds to the starting set of individuals which are to be evolved by the GA. These individuals are usually generated randomly. The population of individuals evolves, via genetic operations, for a certain number of generations. These genetic operations can be of two types, namely mutation and crossover. The mutation GA operators helps to increase population diversity, thus increasing the number of points of the parameter space that are evaluated. The crossover GA operators essentially exchange information between individuals, thus evolving to new and better solutions to the problem being optimized. In general, the parameter space may have many local minima. The GA, by exploring the multidimensional parameter space, jumps between basins, thus avoiding being stuck in a non-global minimum. In order to improve the search for minima, we use, additionally, local minimizers (classical simplex and Monte Carlo) within the basin[25]. This combination, GA in real numbers space and local minimizer, considerably improves the convergence speed, and it has proven to be quite reliable[25,27]. In order to implement the mating or crossover genetic operations the choice of parents is made by random selection method (the roulette wheel method). We also specify the fraction of population that is replaced in each generation and the fraction that remains unchanged. This kind of GA is known as steady-state GA. To produce a new generation we adopt the following genetic operators: four crossover operators (the arithmetic and geometric means, the N and the 2-point crossover) plus the mutation inversion operator as described by Niesse and Mayne[25]. The objective function to be minimized is, of course, the cluster energy and the fitness score is obtained by dynamic linear scaling of the raw objective score in each generation.

For a fixed number N of atoms in the cluster, we performed computations for ten different populations (each of them with 30 individuals). The initial atomic positions were chosen at random under the constraint that the average pair separation be between 0.7 and 1.3 of the bulk distance. The fraction of population that is replaced in each generation adopted was 70%. For $N = 2 - 13$, we used 5000 generations and for $N = 14 - 21$ we used 10000 generations in order to obtain the putative global minimum.

The energy in the GA was computed with the Gupta phenomenological potential[26,28] which was derived from Gupta's expression for the cohesive energy of a bulk material[26] and is based on the second moment approximation to tight binding theory. It is a potential that has a very simple analytical form, which depends on five parameters, and it is written in terms of repulsive pair and attractive many-body terms which are obtained by summation over all atoms.

The explicit functional form for the cohesive energy and the parameter values for Pd used in our calculations are given by Cleri and Rosato.[28] The parameters of the potential for Pd in our model are fitted to bulk properties (cohesive energy, lattice parameter, bulk modulus, independent elastic constants in the appropriate crystal structure at $T = 0$ K), and the vanishing of the energy gradient at equilibrium distance.

B. *ab-initio* DFT pseudopotential calculations

We have performed first-principles DFT calculations using the pseudopotential SIESTA code (Spanish Initiative for Electronic Simulation of Thousand Atoms).[18] This method employs linear combination of pseudo-atomic orbitals as basis sets. The atomic core is replaced by a nonlocal norm-conserving Troullier-Martins[29] pseudopotential that is factorized in the Kleinman-Bilander form[30] and may include nonlinear terms correcting for the significant overlap of the core charges with the valence d orbitals.

To re-optimize the geometrical structures we did a local relaxation using the conjugate gradient algorithm, starting from the structures previously obtained via the genetic algorithm search on a Gupta potential. Simultaneously with the geometrical re-optimization, the SIESTA code allow us to determine the electronic structure for all the different clusters, particularly at the Fermi level which will be used in Kubo's criterion for the determination of the metallic character, and to compare with the results obtained with the TB-recusion method (see below).

In the present calculation, we have used for the exchange and correlation potential the LDA as parameterized by Perdew-Zunger.[31] The ionic pseudo-potentials were generated using the atomic configurations: $4d^9$, $5s^1$ and $5p^0$ for Pd with 2.0, 2.2 and 2.4 a.u. cutoff radii, respectively. The core corrections are included with a radius of 1.2 a.u. We have found from the various pseudo-potentials tested that the $4d^9$, $5s^1$ configuration reproduced slightly better the eigenvalues of different excited states of the isolated Pd atom than the $4d^{10}$, $5s^0$ configuration. Besides, the *ab-initio* electronic occupations of small Pd clusters[32] are closer to this configuration than to the $4d^{10}$, $5s^0$. Valence states have been described using DZP basis sets with two orbitals having different radial

form to describe both the $5s$ and the $4d$ shells of Pd and one orbital to describe the $5p$ shell. We consider an electronic temperature of 25meV and a 120 Ry energy cutoff has been used to define the real space grid for numerical calculations involving the electron density, a larger cutoff does not substantially modify the results.

C. Semiempirical Real-space Tight-Binding calculations

The spin-polarized electronic structure was determined by solving self-consistently a TB Hamiltonian for the $4d$, $5s$ and $5p$ valence electrons in a mean-field approximation. We considered hopping integrals up to third nearest-neighbor distances and fitted to reproduce the band structure of Pd bulk.[33] The changes of the hopping integrals, reflecting in turn the deviation of the interatomic distances (r_{ij}) from their bulk values, were considered, as usual, via the power law of the type $(r_0/r_{ij})^{l+l'+1}$. Here r_0 represents the bulk distance, between first or second neighbors, with l and l' standing for the orbital angular momenta of the electronic states involved in the process.[34] We solve the Hamiltonian in the real space using the recursion method.[34] The number of recursion levels used in our calculation is large enough to assure the stability of the results. The imaginary part of the energy for the calculation of the density of states within the recursion method is chosen so as to correspond to the electronic temperature used in SIESTA. The self-consistent value of the density of states at the Fermi level calculated in this way is used later on for the determination of the nonmetal to metal transition under Kubo's prescription. The local electronic occupation in our TB calculation is fixed by linearly interpolating between the atom and the metal occupations according to the local coordination at site i, and self-consistent potentials are determined to assure the local electronic occupation. We have used [Kr] $4d^9\ 5s^1$ for the electronic configuration of Pd atom. The metal electronic occupations, on the other hand, are 0.60, 0.45, and 8.95 for the s, p, and d electrons of Pd, respectively. The local neutrality approximation has been probed to be a good approximation in transition metal systems[35] and in the present case, atomic and bulk sp and d occupations are mainly the same. The exchange parameter (0.6 eV), which is responsible of the spin-splitting of the electronic states, has been chosen such that reproduces the *ab-initio* DFT calculations of the average magnetic moment of a Pd_{13} icosahedral cluster by Moseler *et al.*[36] and Kumar *et al.*[37] We have chosen the Pd_{13} cluster for the fit because it is the most studied cluster in the literature, and agreement exists concerning its icosahedral geometry.

The same model was used in previous works[19] for the study of Rh clusters and for the study of the single FCC-like Pd clusters.[20] The good agreement with available data in the literature for free clusters, give us confidence in the transferability of the parameterization. The reader

TABLE I: The cluster size (N), average interatomic distance in Å, average coordination number (Z), the symmetry of the Pd_N clusters, and binding energy in eV.

N	Distance	Z	Structure	E_B
2	2.45	2.00	Dumbbell	0.92
3	2.50	2.00	Triangle	1.67
4	2.58	3.00	Tetrahedron	2.17
5	2.62	3.60	Trigonal bipyramid	2.37
6	2.63	4.00	Octahedron (O)	2.58
7	2.66	4.60	Pentagonal bipyramid (PB)	2.65
8	2.64	4.50	O+2	2.75
9	2.67	5.12	PB+2	2.82
10	2.68	5.40	PB+3	2.90
11	2.69	5.64	PB+4	2.96
12	2.70	6.00	PB+5	3.02
13	2.71	6.50	Icosahedron (I)	3.09
14	2.68	6.43	I+1	3.13
15	2.68	6.53	I+2	3.19
16	2.68	6.38	Distorted I-like	3.25
17	2.67	6.67	Distorted I-like	3.30
18	2.67	6.44	Distorted I-like	3.32
19	2.69	7.16	Double Icosahedron (DI)	3.32
20	2.68	6.70	Distorted DI	3.38
21	2.70	7.05	Distorted DI	3.40

can find more details of the model Hamiltonian and of the parameterization in previous works.[19,20]
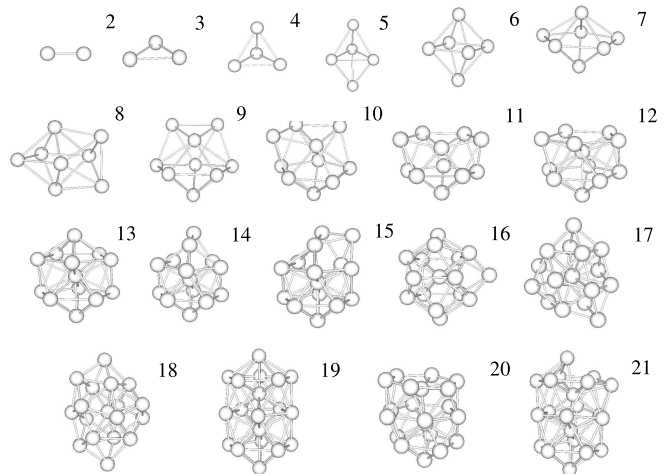
FIG. 1: Ground-state geometrical structures of Pd_N clusters ($2 \leq N \leq 21$) as re-optimized from SIESTA code .

III. GEOMETRICAL STRUCTURES

In Table I, we list the main geometrical properties of the structures of the palladium clusters,[38] illustrated in Fig. 1. In general, we obtain an icosahedral-like growth pattern with some structural disorder, particularly between symmetric closed shell clusters (N =8 to 13, 13 to 19) and for N =20 and 21. For the geometrical properties in Table I, at a given site i within the cluster, we consider as First Nearest Neighbor (FNN) those atoms located at distances within 0.85 to 1.15 of the bulk interatomic one. The structural disorder in our clusters (is reflected by a wide distribution in the interatomic distance) results from the fully unconstrained relaxation process. Slightly non-symmetrical arrangements are obtained for the closed shell clusters. For the symmetric closed shell clusters there are two and three well defined interatomic distances.

Let us briefly comment on these geometrical structures in comparison with other geometries reported in the literature. In the case of $N \leq 13$, Futschek[39] report Pd clusters that can be seen as relaxed fragments of the fcc crystal bulk structure, whereas ours are mainly non-crystalline structures, particularly in the range of $7 \leq N \leq 13$, in which five fold symmetry is observed. Our geometrical structure are more similar to those reported by Kumar[37], for $N = 2 - 15$ and 19. For the rest of the clusters their structures are icosahedral-like. In our case, for $N = 16 - 18, 20$ and 21, the structures have some structural disorder as previously quoted. Otherwise they are also icosahedral-like. In general, when our geometries coincide with those reported by Futschek et al. and Kumar et al. the interatomic distances of the clusters are very similar (within 2%).

Concerning the binding energy, we have a monotonic increasing dependence with the cluster size like Kumar and coworkers.[37] although our calculated values overestimate the GGA ones. This overestimation is expected since it is well know that the LDA approximation give larger binding energy than GGA. The binding energy in our calculation is given approximately by $E \approx E_0 Z^{1/3}$, been E_0 a constant that depends on the approximation used.

IV. METALLICITY

We use Kubo's criterion as one of the simplest approximations to estimate the nonmetal-metal transition. This criterion establishes that a system becomes metallic when the average spacing between the electronic levels within the cluster becomes smaller than $k_B T$ and the discrete energy levels begin to form a quasi-continuous band, or formulated in terms of the electronic density of states $D_N(E)$, when $D_N(E)$ at the Fermi level exceeds the $1/k_B T$ value.[16] Notice that experiments are usually performed at finite T and the broadening of the $T = 0$ calculated electronic spectrum reflects in a first

approximation the finite temperature effects. Therefore, for the metallic character to be accurately determined it is necessary to correctly account for the position of the electronic states in the neighborhood of the Fermi level. In this sense, it requires a more accurate determination of the environment-dependent electronic structure than that required for the magnetic properties. We compare the real-space TB model that takes advantage of the recursion method and the SIESTA code. Since the TB Hamiltonian is solved here using the recursion method we directly obtain the density of states but not the eigenfunctions Kubo's criterion allows to compare TB and the SIESTA without the need of the TB spectrum.

We have also considered the Friedel's square d band model based on the second moment approximation[12,40] in order to enrich the discussion. Friedel's model is very simple and depends only on average coordination number ($Z(N)$) to determine the d-band width and the $D_N(E)$ at the Fermi level through the second moment approximation. In this model the s and p electrons are not considered and a rectangular shape is assumed for the d-band, in which the total $D_N(E)$ at the Fermi is $10N/W(N)$. The second moment approximation introduces a dependence of the band width $W(N)$ on the local coordination number, the band width of a finite size N cluster is given by $W(N) = W_B(Z(N)/Z_B)^{1/2}$, where W_B and Z_B are the band width and the bulk coordination number, respectively.[41]
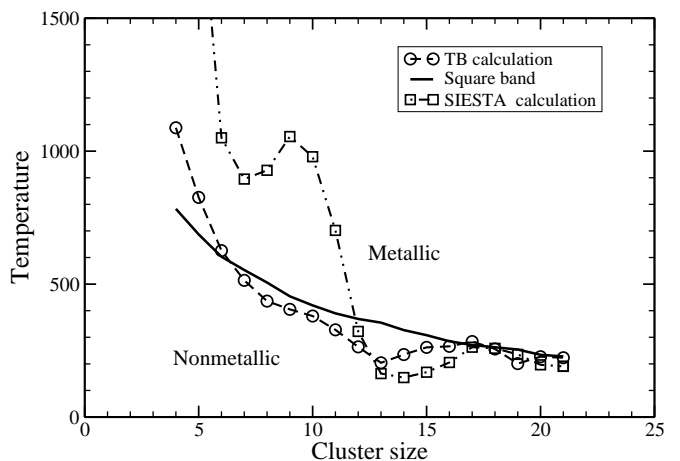
FIG. 2: Metallicity temperature as a function of the cluster size from TB and SIESTA calculations. We also provide results from Fridel's model.

In Fig. 2 we present the results of our TB and SIESTA calculations, together with the more crude estimation obtained using the Friedel's d-band model. The results split the temperature range in two parts, the low temperature or non-metallic region and the high temperature or metallic region. A cluster with a temperature below the line (within the different models) behaves as an insulator whereas above the line it exhibits a metallic character.

In general, the results for the metallicity indicate, as

expected, that the larger is the cluster the lower is the temperature required for its becoming metallic. In the case of Friedel's model, we have a monotonic decreasing dependence, consistent with the fact that this model only takes into account the average coordination in the determination of the $D(E)$ at the Fermi level no details of the symmetry of the cluster geometry are taken into account (beyond the average coordination number).[12,13,41] With the TB model, we obtain a decreasing dependence but with more structure. We have a smooth shoulder around $N = 8$ and two shallow local minima at $N = 13$ and $N = 19$ indicating that these clusters are more metallic than their neighbor cluster sizes of the same icosahedral family.

With SIESTA we obtain a richer structure than with TB, with well defined minima at $N = 7, 13 - 14, 20 - 21$ and maxima at $N = 9, 17 - 18$; a minimum (maximum) indicates, again, a more metallic (insulator) character in comparison with its neighbor cluster sizes can be observed. The richer structure obtained with SIESTA is mainly due to its more accurate description of the HOMO-LUMO gap. In general, the largest the gap the largest the temperature required to have metallic-like character. However it is remarkable that the TB calculation is able to reproduce the same trend as the DFT SIESTA code for clusters larger than only $N \approx 12$, despite the fact that the TB model is, in principle, better adapted to large systems.

Experimental results by Aiyer and coworkers[5] based on tunneling conductance measurements of Pd clusters supported on graphite indicate that, at room temperature, clusters of $N \approx 50$ are in the threshold to undergo a nonmetal-metal transition. This experimental observation is endorsed by the different reactivities shown for the Pd_{50} clusters in comparison with larger Pd clusters.[5] However, by performing core-level binding energy shift measurements, Wertheim[4] predicts that the insulator-metal transition at room temperature for Pd clusters (supported on amorphous carbon) is in the range of 7 to 10 Å (about 20 to 50 atoms) suggesting that the metallicity could be present at even smaller sizes than the ones reported by Aiyer et al.

We performed additional TB calculations for a $N = 55$ icosahedral Pd cluster with bulk interatomic distances (this cluster size is easily handled within the TB code),

and we obtained a metallicity temperature of ≈ 70 K. This result is consistent with both experimental observations in the sense that clusters of this size should present metallic behavior at room temperature. The results of Fig. 2 for $N \approx 20$ are supported by Wertheim's[4] measurements that find metallicity in Pd clusters of very small sizes. It is worth noticing that nonmetal-metal transition for supported Fe clusters on GaAs has been reported also at very small sizes, such as $N \approx 35$ atoms at room temperature.[6]

V. CONCLUSIONS

We have performed a systematic study of the metallicity of Pd_N $(2 \leq N \leq 21)$ clusters using: the *ab-initio* pseudopotential DFT method, as implemented in the SIESTA code, and a self-consistent real space *spd* TB method. We find that for the metallic character, whose determination requires to accurately account for the position of the electronic states close to the Fermi level, the DFT approximation is more reliable than the TB, although it is remarkable that the TB calculation is able to reproduce the same trend as the DFT SIESTA code for clusters larger than only $N \approx 12$, despite the fact that the TB model is better adapted to large systems.

The results for the nonmetal-metal transition studied using the Kubo's criterion are consistent with tunneling conductance measurements of Pd clusters supported on graphite[5] and with core-level binding energy shift measurements[4], which predict that the insulator-metal transition at room temperature for Pd clusters is in the range of 20 to 50 atoms.

[1] Fröhlich H., (1937) Physica (Utrecht) **4**, 406.

[2] N. Agräit, A.L. Yeyati, and J.M. Ruitenbeek, (2003) Phys. Reports Lett. **377**, 81.

[3] A. R. Rocha, V.M. García-Suárez, S.W. Bailey, C.J. Lambert, J. Ferrer and S. Sanvito, (2005) Nature Mat. **4**, 335.

[4] Wertheim G. K., (1989) Z. Phys. D **12**, 319.

[5] Aiyer H. N., Vijayakrishnan V., Subbanna G. N., and Rao C. N. R., (1994) Surf. Sci. **313**, 392.

[6] First P. N., Stoscio J. A., Dragoset R. A., Pierce D. T., and Celotta R. J., (1989) Phys. Rev. Lett. **63**, 1416.

[7] Rademann K., Kaiser B., Even U., and Hensel F., (1987) Phys. Rev. Lett. **59**, 2319.

[8] Parks E. K., Klots T. D., and Riley S. J., (1990) J. Chem. Phys. **92**, 3813.

[9] Dai Y., Dai D., Hung B., and Yan C., (2005) Eur. Phys. J. D **34**, 105.

[10] Wang J., Wang G., and Zhao J., (2003) Phys. Rev. B **68**, 013201.

[11] Zhao J., Chen X., and Wang G., (1994) Phys. Rev. B **50**, 15424.

[12] Aguilera-Granja F., Bouarab S., Vega A., Alonso J. A., and Montejano-Carrizales J. M., (1997) Solid State Comm. **104**, 635.

[13] Aguilera-Granja F., Montejano-Carrizales J. M., Guevarra J., and Llois A. M., (2000) Solid State Comm. **113**, 147.

[14] Guirado-López R. and Aguilera-Granja F., (2000) Phys. Lett. A **265** , 116.

[15] Wang Q., Sun Q., Yu J. -Z., and Kawazoe Y., (2001) Solid State Commun. **117**, 635.

[16] Kubo R., Kawabata A., and Kobayashi S., (1984) Ann. Rev. Mat. Sci. **14**, 49.

[17] G. Barcaro, A. Fortunelli, G. Rossi, F. Nita, R. Ferrando, (2007) Phys. Rev. Lett. **98**, 156101.

[18] Soler J. M., Artacho E., Gale J. D., García A., Junquera J., Ordenjon P., and Sánchez-Portal D., (2002) J. Phys.: Condens. Matter **14**, 2745.

[19] Aguilera-Granja F., Rodríguez-López J. L., Michaelian K., Berlanga-Ramírez E. O., and Vega A., (2002) Phys. Rev. B **66**, 224410.

[20] Aguilera-Granja F., Montejano-Carrizales J. M., and Vega A., (2004) Phys. Lett. A **332**, 107.

[21] Holland J., *Adaptation in Natural and Artificial Systems*, (University of Michigan Press, Ann Arbor, MI, USA, 1975).

[22] Goldberg D.E., *Genetic Algorithms in Search, Optimizations & Machine Learning*, (1989 Addison-Wesley, Reading, MA, USA).

[23] Mitchell M., *An Introduction to Genetic Algorithms*, (1998 MIT Press, Cambridge, MA, USA).

[24] Deaven D. M.,Tit N., Morris J. R., and Ho K. M., (1996) Chem. Phys. Lett. **256** 195.

[25] Niesse J. A. and Mayne H. R., (1996) J. Chem. Phys. **105**, 4700.

[26] Gupta R. P., (1985) Phys. Rev. B **23**, 6265.

[27] Iwamatsu M., (2000) J. Chem. Phys. **112**, 109760.

[28] Cleri F. and Rosato V., (1993) Phys. Rev. B **48**, 22.

[29] Troullier N. and Martins J. L., (1991) Phys. Rev. B **43**, 1993.

[30] Kleinman L. and Bilander D. M., (1982) Phys. Rev. Lett. **48**, 1425.

[31] Perdew J. and Zunger A., (1981) Phys. Rev. B **23**, 5048.

[32] Aguilera-Granja F., Vega A. and Ferrer J., (2006) Phys. Rev. B **74** , 174416.

[33] Papaconstantopoulos D. A., *Handbook of the Band Structure of Elemental Solids* (Plenum, New York, 1986).

[34] Haydock R., *Solid State Physics*, edited by E. Ehrenreich, F. Seitz, and D. Turnbull, Vol. 35, (Academic Press, London, 1980), p. 215.

[35] Martínez E., Robles R., Vega A., Longo R. C., and Gallego L. J., (2005) Euro. Phys. J. D **34**, 51.

[36] Moseler M., Häkkinen H., Barnett R. N., and Landman Uzi, (2001) Phys. Rev. Lett. **86**, 2545.

[37] Kumar V. and Kawazoe Y., (2002) Phys. Rev. B **66**, 144413.

[38] Rogan J., García G., Valdivia J. A., Orellana W., Romero A. H., Ramírez R., and Kiwi M., (2005) Phys. Rev. B **72**, 115421.

[39] Futschek T., Marsman M., and Hafner J., (2005) J. Phys.: Condens. Mat. **17**, 5927.

[40] Harrison W. A., *Electronic Structure and the Properties of Solids* (1980 Freeman, San Francisco).

[41] Tomanek D., Mukherjee S., and Benneman K. H., (1983) Phys. Rev. B **28**, 665.